Chinese Chemical Letters 36 (2025) 110076

Contents lists available at ScienceDirect

Chinese Chemical Letters

journal homepage: www.elsevier.com/locate/cclet

Copper-catalyzed and biphosphine ligand controlled 3,4-boracarboxylation of 1,3-dienes with carbon dioxide

He Yao[a,1], Wenhao Ji[a,1], Yi Feng[a], Chunbo Qian[a], Chengguang Yue[a], Yue Wang[a], Shouying Huang[a,b], Mei-Yan Wang[a,b,*], Xinbin Ma[a,*]

[a] School of Chemical Engineering and Technology, Key Laboratory for Green Chemical Technology of Ministry of Education, Collaborative Innovation Center of Chemical Science and Engineering, Tianjin University, Tianjin 300072, China
[b] Ningbo Key Laboratory of Green Petrochemical Carbon Emission Reduction Technology and Equipment, Zhejiang Institute of Tianjin University, Ningbo 315200, China

ARTICLE INFO

Article history:
Received 16 April 2024
Revised 15 May 2024
Accepted 30 May 2024
Available online 31 May 2024

Keywords:
Carbon dioxide
Ligand effect
Carboxylation
β,γ-Unsaturated carboxylic acid
DFT calculation

ABSTRACT

A strategy for copper-catalyzed and biphosphine ligand controlled boracarboxylation of 1,3-dienes and CO_2 with 3,4-selectivity was developed. The CuCl coupled with DPPF (1,1′-bis(diphenylphosphino)ferrocene) was assigned to be the best catalyst, with 84% yield and exclusive 3,4-selectivity. The ligand effect on both catalytic activity and regioselectivity of boracarboxylation was disclosed, which is rarely reported in any copper catalyzed boracarboxylation. The borocupration process is revealed to be a vital step for the biphosphine participated boracarboxylation of 1,3-dienes with CO_2. The minimal substrate distortion occurring in 3,4-borocupration favors the 3,4-regioselectivity of boracarboxylation. The "pocket" confinement and suitable β_n (92°–106°) of bisphosphine ligands are demonstrated to be in favour of the interaction between LCu-Bpin complex (the catalytic precursor) and 1,3-diene substrate to decrease their interaction energy $\Delta E_{int}(\zeta)$ in 3,4-borocupration, thus promoting the 3,4-boracarboxylation.

The usage of CO_2 as a low-cost and renewable C1 building block for the synthesis of value-added chemicals is of great importance and has attracted increasing interest [1-9]. The carboxylation of carbon nucleophiles with CO_2 is a straightforward protocol for the synthesis of carboxylic acids [10-16]. It was recently demonstrated that β,γ-unsaturated carboxylic acids, which are important motifs in varieties of bioactive molecules and useful intermediates for organic synthesis, can be obtained by the carboxylation of 1,3-dienes with CO_2. While one of the most challenges for carboxylation of 1,3-dienes with CO_2 is how to control the regioselectivity. In this regard, elegant efforts on transition metal (*i.e.*, Ni [17-19] and Cu [20–22]) catalyzed 1,4-selective carboxylation of 1,3-dienes with CO_2 were achieved (Scheme 1A, a and b). Electrochemical [23-25] and photochemical [26] approaches have also been demonstrated to be efficient for the control of 1,4-selectivity (Scheme 1A, a, c and d). The regioselectivity in 1,2-carboxylation was finely realized *via* a copper catalyzed two-step procedure [27,28] and Grignard reagent involved titanocene catalysis (Scheme 1B) [29]. Despite the elegant advances realized, rarely studies for the 3,4-selective carboxylation of 1,3-dienes with CO_2 were present. Iwasawa [30] and Li [26] achieved the 3,4-hydrocarboxylation *via* palladium catalysis and photochemical protocol respectively, while the regioselectivity tends to depend on the substrate employed or organometallic reagent is required (Scheme 1C, g).

Here, we developed an efficient strategy for boracarboxylation of 1,3-dienes and CO_2 with high level of 3,4-selectivity using a copper(I)/biphosphine catalyst (Scheme 1C, h). Although the copper catalyzed boracarboxylation of unsaturated hydrocarbons has been extensively investigated [31-34], the exclusive 3,4-boracarboxylation of 1,3-dienes with CO_2 has not been reported. The previous research on hydro/heteroboration [35-40] and boracarboxylation [41-45] of unsaturated hydrocarbons which primarily focused on catalyst system construction and the optimization of reaction conditions, as well as the investigation of reaction intermediates, provide lots of inspiration for the establishment of our reaction protocol in this work. However, the underlying reaction mechanism, such as the key steps, the evolution of reactants, and the intrinsic effect of phosphine ligand, remains undisclosed in terms of how the catalyst influences both activity and selectivity.

* Corresponding authors.
E-mail addresses: mywang2017@tju.edu.cn (M.-Y. Wang), xbma@tju.edu.cn (X.B. Ma).
[1] These authors contributed equally to this work.

https://doi.org/10.1016/j.cclet.2024.110076
1001-8417/

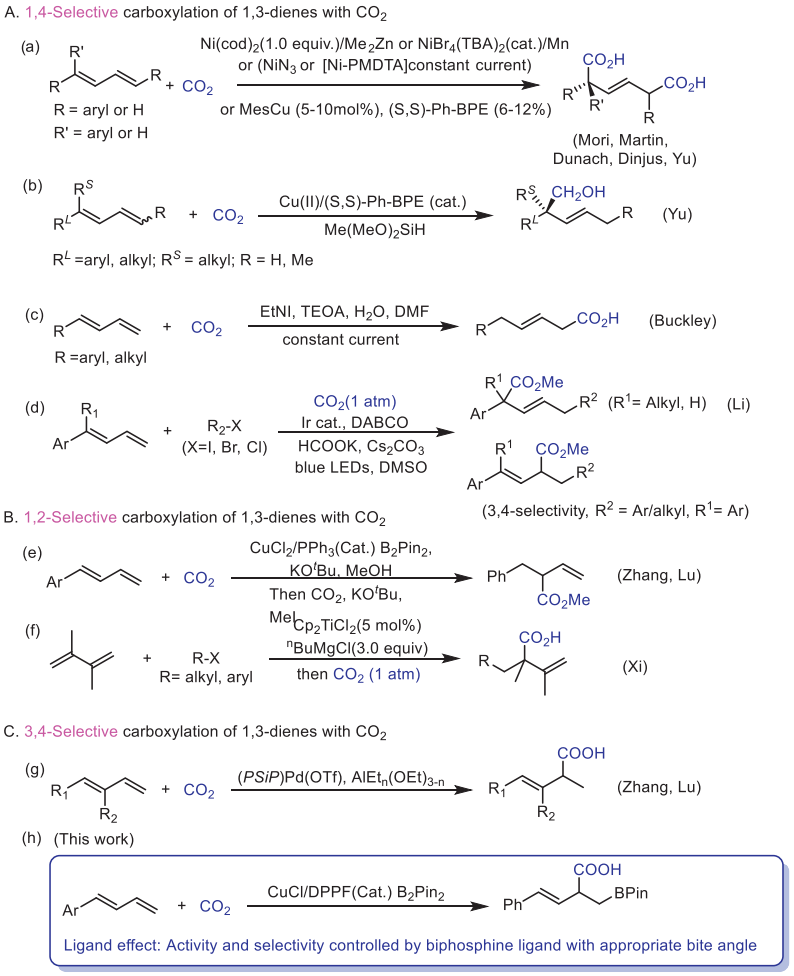

Scheme 1. Carboxylation of 1,3-dienes and CO_2 with specific regioselectivity.

On the basis of the established method of copper(I)/biphosphine catalyzed boracarboxylation of 1,3-dienes, we also explored the structure-activity relationship of Cu(I)/bisphosphine complex by a combination of experimental and theoretical analysis, focusing on the influence of different bisphosphine ligands on the activity and 3,4-selectivity of boracarboxylation. Considering the joint influence of ligands' electronic and steric effects, the descriptor of bite angle (β_n) between copper and phosphorus atoms in the catalytic precursor of LCu-Bpin complex was introduced [46]. It is revealed that the low substrate distortion in 3,4-borocupration contributes the regioselectivity of 3,4-boracarboxylation. The "pocket" confinement and suitable β_n (92°–106°) of bisphosphine ligand are demonstrated to be conducive to the interaction between LCu-Bpin complex and 1,3-dienes substrate, facilitating the 3,4- borocupration process, thereby promoting the 3,4-boracarboxylation of 1,3-dienes with CO_2.

To eliminate the influence of substituent steric hindrance on the experiment, we began our investigation by using 1-aryl-1,3-butadiene as the model substrate to react with B_2pin_2 and CO_2. A range of biphosphine ligands coupled with CuCl were tested to evaluate the reactivity of boracarboxylation of **1a** with CO_2. All the investigated biphosphine ligands exhibited exclusive selectivity towards the 3,4-boracarboxylation product (**2a**). For ligands with flexible alkyl chains, the length of the chain affects the catalytic activity to some extent (Table 1, entries 1–6). The ligands with C3 to C5 chain length showed better catalytic efficiency, of which (*R*,*R*)-DIOP gives **2a** in 70% yield (entry 6). Rigid biphosphine ligands with phenyl or biphenyl backbones performed in poor catalytic activity (entries 7–9), while the BINAP could achieve **2a** in 68% yield (entry 10), perhaps due to its suitable distance of two P atoms. Rigid Xantphos and NiXantphos ligands also afford poor yield (entries 11 and 12). The ligand DPE Phos with similar but relatively flexible backbone to Xantphos delivers 45% yield (entry 13). Subsequently, a series of ferrocene-based ligands were examined (entries 14–16), among which DPPF was demonstrated to be the best choice with a yield of 84%. The excellent performance of DPPF may be attributed to its specific ferrocene backbone and good electron-donating ability [47]. The monodentate ligand PPh_3 was also examined, none of the 3,4-boracarboxylation product was detected (entry 17).

To demonstrate that this protocol could employ the readily available 1,3-dienes to produce 4-phenyl-β,γ-unsaturated acid derivatives, we then examined the 3,4-boracarboxylation of various 1,3-dienes with CuCl/DPPF as a catalyst under the optimized conditions (Scheme 2). In general, 1-aryl substituted 1,3-butadienes could give the corresponding boracarboxylation products with absolute 3,4-selectivity. Modest to good yields were obtained using electron-rich 1-aryl substituted 1,3-butadiene (**2b-2f**). Notably, the *ortho*- and *meta*-substituents did not affect the efficiency of this transformation (**2b**, **2c**). Heterocyclic substrate such as 1-thienyl-1,3-butadiene worked well under this reaction condition (**2g**). When halogen-substituted aromatic 1,3-dienes were employed as starting materials, the corresponding products could be afforded, which could be used for further transformation (**2h**, **2i**). 1-Aryl

Table 1
Various Cu(I)/biphosphine ligands catalyzed 3,4-boracarboxylation of **1a** with CO_2.[a]

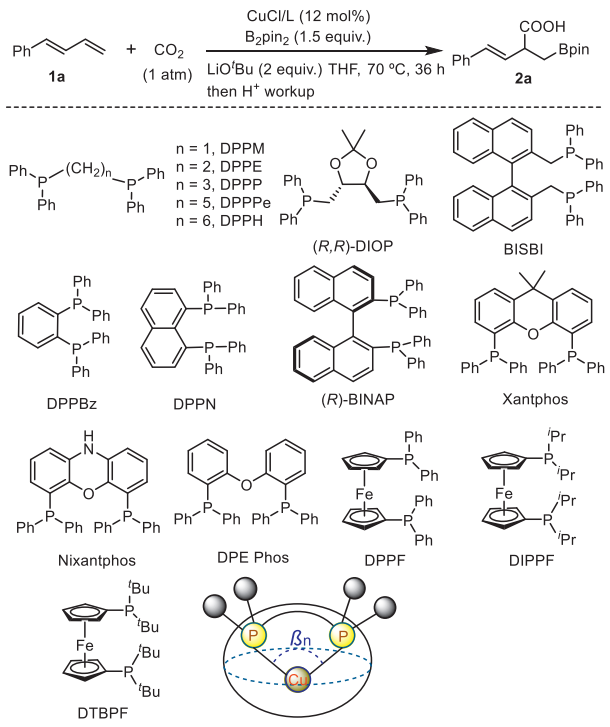

Entry	Ligand	Yield (%) [b]	β_n (°) [c]
1	DPPM	15	-[d]
2	DPPE	18	85
3	DPPP	65	92
4	DPPPe	43	103
5	DPPH	12	-[d]
6	(*R*,*R*)-DIOP	70	102
7	BISBI	26	110
8	DPPBz	16	82
9	DPPN	22	86
10	(*R*)-BINAP	68	95
11	Xantphos	25	109
12	NiXantphos	18	114
13	DPE Phos	45	106
14	DPPF	84	100
15	DIPPF	25	113
16	DTBPF	23	111
17	PPh_3	None	-[d]

[a] Reaction conditions: **1a** (0.033 g, 0.250 mmol), CuCl (0.003 g, 0.030 mmol), ligand (0.030 mmol), B_2pin_2 (0.095 g, 0.375 mmol), LiO^tBu (0.040 g, 0.500 mmol), THF (3 mL), CO_2 (99.999 %, 1 atm, closed), 70 °C, 36 h, then workup using 8 mL 1 mol/L HCl.
[b] Isolated yield.
[c] The value of β_n was obtained *via* DFT calculation.
[d] The β_n was not optimized out.

substituted 1,3-diene bearing strong electron withdrawing group such as CF_3 (**2j**) was viable for this reaction. The reactivity of 2- and 3-substituted 1,3-butadiene were also explored, but the regioselectivity needed further improvement.

To understand the reaction mechanism and ligands' effect on the reactivity and selectivity, a theoretical analysis was then employed [48-52]. The DPPP with good activity and small geometric structure was selected as a model ligand to simplify computational work [53]. Extensive conformational searches were performed to calculate the energy distribution along the boracarboxylation reaction pathways, as depicted in Fig. 1. The results indicate that the borocupration (1-phenyl-1,3-butadiene reacts with DPPPCu-Bpin complex to deliver intermediate **INT2** *via* a transition state **TS1**) is the rate-determining step and a crucial process governing the regioselectivity of the boracarboxylation reaction [54-56]. Among all potential borocupration pathways, the 3,4-borocupration exhibits the lowest barrier to overcome, giving the intermediate **INT2a** (for details of energy distribution analysis of various borocupration pathways, please see Fig. S4 in Supporting information). The **INT2a** further undergoes 1,3-copper migration to generate intermediate **INT2a'** which is more thermodynamically stable. CO_2 insertion into the Cu-C bond of intermediates **INT2a** and **INT2a'** may occur through a trimeric or hexameric cyclic transition state [22,57]. It is revealed that CO_2 coupling to the C3 position of **INT2a'** *via* **TS3a**, a hexameric cyclic transition state, is energetically favored. This is consistent with the experimental results, where the primary product is identified as the 4,3-boracarboxylation compound.

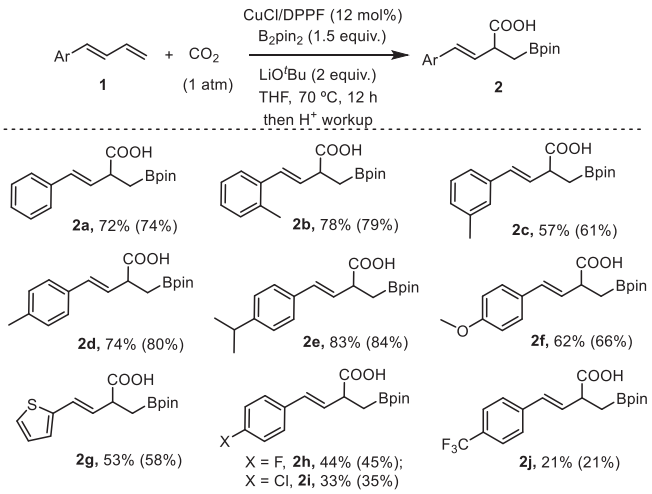

Scheme 2. Scope of 1-aryl-1,3-butadienes. Reaction conditions: **1** (0.250 mmol), CuCl (0.003 g, 0.030 mmol), DPPF (0.017 g, 0.030 mmol), B_2pin_2 (0.095 g, 0.375 mmol), LiO^tBu (0.040 g, 0.500 mmol), THF (3 mL), CO_2 (99.999 %, 1 atm, closed), 70 °C, 12 h, then workup using 8 mL 1 mol/L HCl. Isolated yield. The yields in brackets were determined by ^1H NMR technique using 1,1,2,2-tetrachloroethane as initial standard.

To get insight into the energy differences, the distortion/interaction-activation strain analysis (DIAS), also called the activation strain model, was conducted to the borocupration. In this model, the activation energy $\Delta E(\zeta)$ is decomposed into the distortion energy term (ΔE_{strain}) and the interaction energy term (ΔE_{int}): $\Delta E(\zeta) = \Delta E_{strain} + \Delta E_{int}$ [58,59]. The distortion energy, which is related to the structural distortion that reactants (1-phenyl-1,3-butadiene and LCu-Bpin) deform from equilibrium geometries to fragments in transition structures (**TS1**), is decomposed into ΔE_{strain}(diene)(ζ) (Fig. 2, red bar) and ΔE_{strain}(LCu-Bpin)(ζ) (green bar). The interaction energy $\Delta E_{int}(\zeta)$ (blue bar) is the energy of the combination of the two distorted reactants to adjust their electronic structure. As shown in Fig. 2, with a similar ΔE_{strain}(LCu-Bpin)(ζ) for the four transition states (**TS1-12**, **TS1-21**, **TS1-34**, and **TS1-43**), the lowest $\Delta E(\zeta)$ (black bar) for **TS1-34** is attributed to the lowest distortion energy ($\Delta E_{strain(diene)}(\zeta) = 22.0$ kcal/mol) of 1-phenyl-1,3-butadiene. The results indicate that the regioselectivity of borocupration procedure is determined by the degree of substrate distortion during the interaction with the catalyst. Minimal substrate distortion occurs when the borocupration undergoes on the C3 and C4 positions of 1-phenyl-1,3-butadiene, thus giving priority to 3,4-regioselectivity.

Having obtained the energy distribution of the boracarboxylation reaction and the most favorable 3,4-regioselectivity, the ligand effect on diversity of catalytic activities that different Cu(I)/biphosphine complexes showed was then explored *via* the frontier molecular orbital theory. The frontier molecular orbitals of

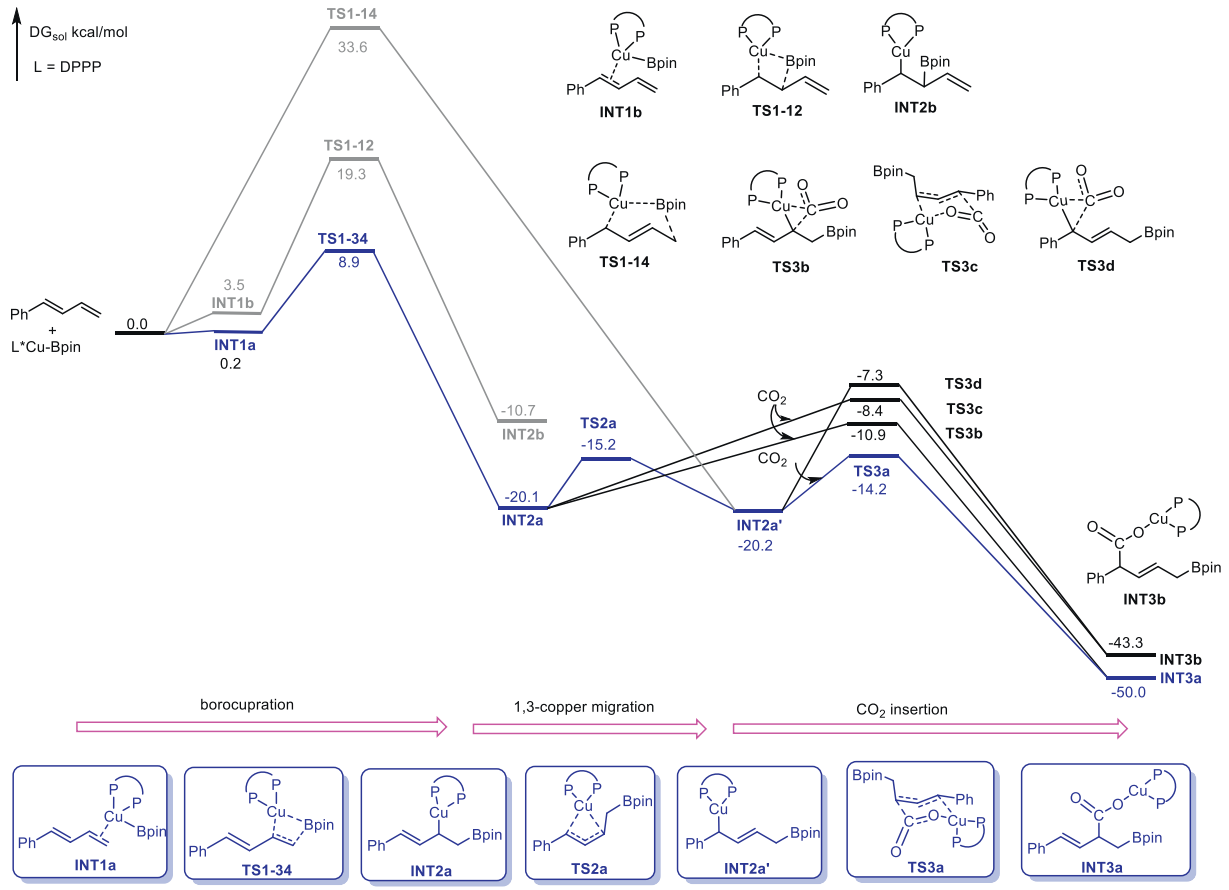

Fig. 1. Energy profiles of Cu(I)/DPPP catalyzed boracarboxylation of 1-phenyl-1,3-butadiene with CO_2.

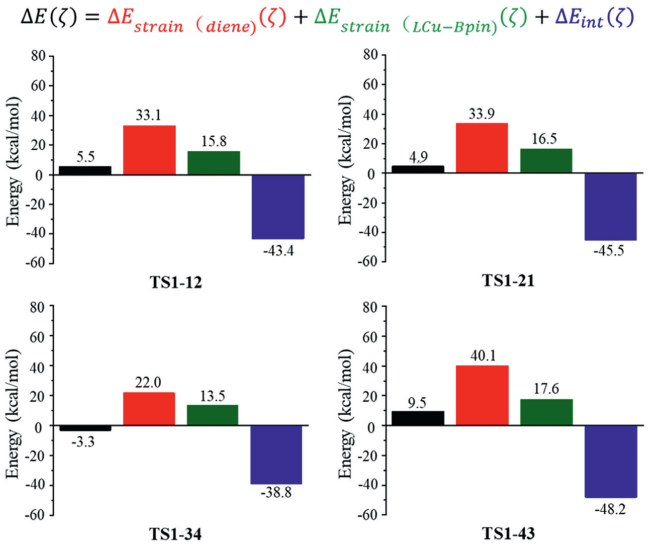

Fig. 2. DIAS analysis on four transition states of borocupration.

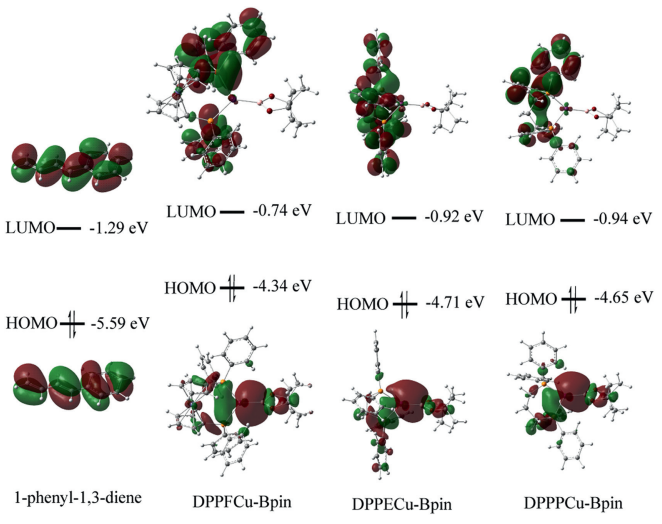

Fig. 3. Frontier molecular orbitals were calculated for 1-phenyl-1,3-butadiene and LCu-Bpin species.

1-phenyl-1,3-butadiene and LCu-Bpin species are shown in Fig. 3 [60,61]. It is revealed that the energy gap between the HOMO orbital of DPPFCu-Bpin complex (σ orbital) and the LUMO orbital of 1-phenyl-1,3-butadiene (π^* orbital) is strikingly small, enabling the ligand of DPPF more favorable for the 3,4-borocupration process than other ligands, thus facilitating the followed 3,4-boracarboxylation more efficiently.

To further dissect the influence of different bisphosphine ligands on the 3,4-borocupration, DIAS analysis on the transition states of 3,4-borocupration that four representative ligands participated, expressed as **TS1-34-DPPE**, **TS1-34-DPPP**, **TS1-34-DPPF**, and **TS1-34-DIPPF**, were carried out. The result indicates that the energy difference in 3,4-borocupration is predominantly determined by the interaction energy $\Delta E_{\text{int}}(\zeta)$ between the distorted catalyst and substrate (Fig. 4).

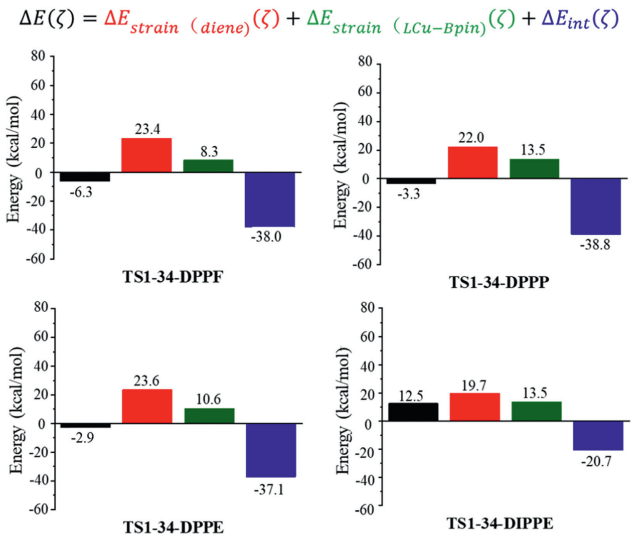

Fig. 4. DIAS analysis on transition states of four representative ligands participated 3,4-borocupration.

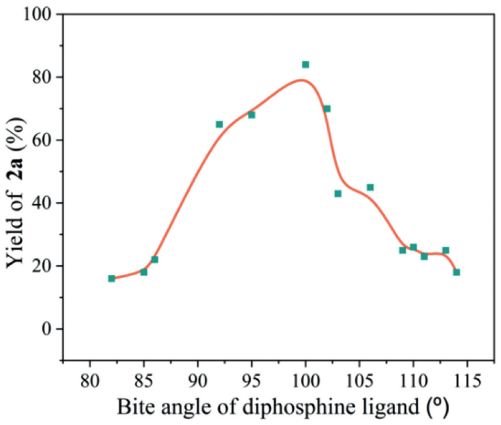

Fig. 6. The relation curve of bite angles with yields.

Although most backbones of ligands do not significantly change the geometry of the substrate, the interaction between the substrate and ligand could assist the transformation of the substrate toward transition state [62]. Hence, the steric effect of bisphosphine ligand could affect the reaction crucially. A series of structural parameters for LCu-Bpin complexes used in experiments were extracted based on the optimal structures, and the percent buried volume ($\%V_{bur}$) of the bisphosphine ligand in each LCu-Bpin complex was calculated [63]. DPPM and DPPH coordinated with the copper center in η^1 coordination mode show small space occupation due to their high flexibility of the skeleton. The DPPF with the best catalytic performance exhibits the highest $\%V_{bur}$ (61.7%). But a higher $\%V_{bur}$ does not imply greater catalytic activity [64]. Hence, in-depth analysis of the spatial configurations was then performed to generate the ligand steric maps (Fig. S5 in Supporting information). The steric maps of LCu-Bpin complexes composed of DPPP, BINAP, DIOP, and DPPF, which exhibit high catalytic activity (yield over 65%), present a "pocket" shape (Figs. 5a-d). However, ligands such as DPPM, DPPH, DPPBz, and DPPE, exhibit less-confined spatial (Figs. 5e-h), resulting in negative effect on the reaction. These results indicate that the "pocket" shaped bisphosphine ligands could offer confined spatial to accept and lock the substrate effectively to facilitate the transformation of 1-phenyl-1,3-butadiene toward transition state in 3,4-borocupration, thus promoting the 3,4-boracarboxylation of 1-phenyl-1,3-butadiene with CO_2.

Taking both electronic and steric effect into account, the bite angle (β_n), a comprehensive reflection of the electronic and steric effect of the bisphosphine ligand, was also introduced and valued by DFT calculation. The relationship between β_n and the reactivity of 3,4-boracarboxylation was investigated, as illustrated in Table 1 and Fig. 6. The LCu-Bpin complexes with β_n among 92°–1 06° shows benign catalytic activity, while too large (≥109°) and too small (≤86°) β_n are not conducive to the reaction. The structure-activity relationship based on β_n is consistent with that of steric hindrance of ligand. In fact, the macroscopic embodiment of β_n is still a steric hindrance affected by the electronic effect. Therefore, it may be explained by that the LCu-Bpin complex with small β_n ligand is not enough to interact with substrate to drive the substrate distortion, while excessively large β_n supplies weak coordination of substrate to Cu center [66].

Finally, the influences of different ligands on energy barriers of the rate-determining step, *i.e.*, 3,4-borocupration, were studied (Fig. 7). Among the selected ligands of DPPE, DPPP, DPPF and DIPPF, the DPPF with an optimal β_n (100°) gives the smallest energy barrier for 3,4-borocupration (8.6 kcal/mol), enabling the 3,4-boracarboxylation of 1-phenyl-1,3-butadiene with CO_2 proceeds tenderly. This further illustrates an appropriate β_n is conducive

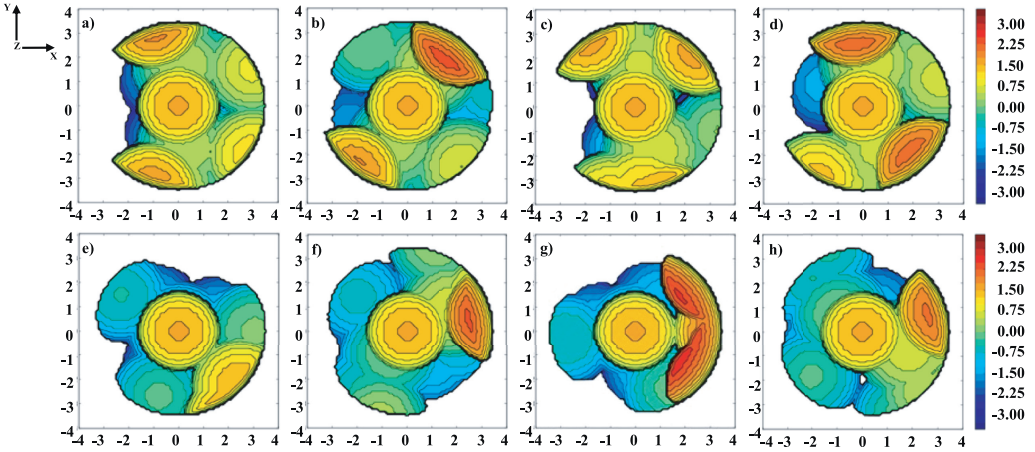

Fig. 5. Steric maps of (a) DPPP, (b) BINAP, (c) DIOP, (d) DPPF, (e) DPPM, (f) DPPH, (g) DPPBz, (h) DPPE. The unit of color code is Å. The plane of the Cu atom is horizon and the steric maps are viewed down the z axis. The red and blue zones indicate the more- and less-hindered zones in the catalytic pocket, respectively. Catalytic pocket images were generated with SambVca 2.1 [65].

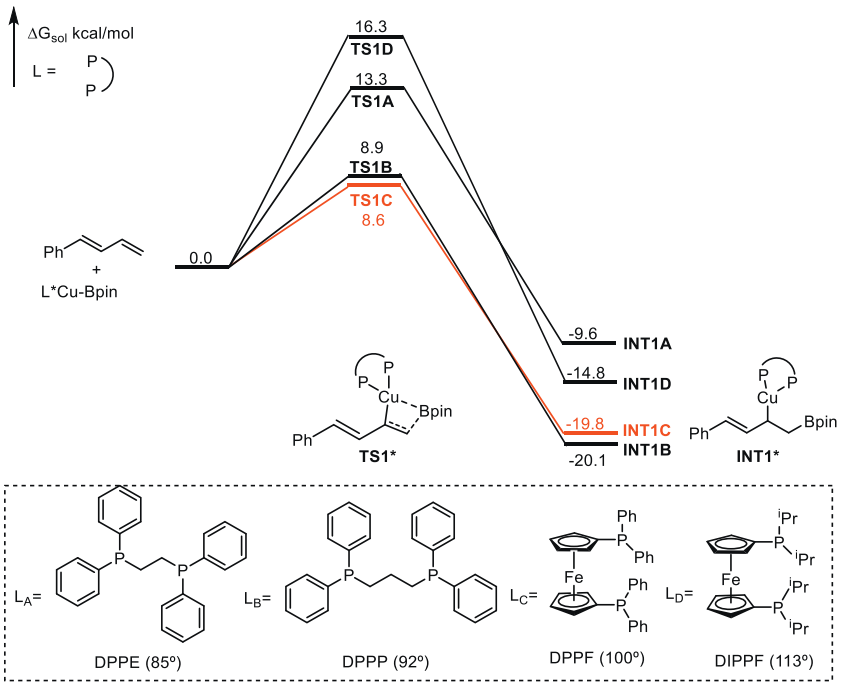

Fig. 7. Energy profiles of the formation Cu(I)/bisphosphine-catalyzed borocupration of 1-phenyl-1,3-butadiene.

to the interaction of the LCu-Bpin complex and substrate to decrease the interaction energy $\Delta E_{\text{int}}(\zeta)$, thus facilitating the 3,4-boracarboxylation.

In this work, we developed an intriguing strategy for copper-catalyzed and biphosphine ligand controlled 3,4-borocarboxylation of 1,3-dienes with CO_2. Among various biphosphine ligands evaluated, DPPF emerged as the most effective, showcasing up to 84% yield of 4-phenyl-2-((Bpin)methylene)but-3-enoic acid and absolute regioselectivity. The ligand effect is revealed to be significant for the reactivity and selectivity *via* experiment and theoretical analysis. The borocupration process is dedicated to be a rate-determining step for biphosphine participated boracarboxylation of 1,3-dienes with CO_2. The minimal substrate distortion occurring in 3,4-borocupration favors the 3,4-regioselectivity of boracarboxylation. On the other hand, the high activity of DPPF is attributed to its optimal bite angle (100°) and "pocket" confinement structure presented in the catalytic precursor of the DPPFCu-Bpin complex, which is in favor of the interaction between the DPPFCu-Bpin and 1,3-diene substrate to decrease their interaction energy $\Delta E_{\text{int}}(\zeta)$ in 3,4-borocupration, thus promoting the 3,4-boracarboxylation. Such findings may be of great interest to the rational design of ligands in various biphosphine involved catalytic reactions.

Declaration of competing interest

The authors declare that they have no known competing financial interests or personal relationships that could have appeared to influence the work reported in this paper.

CRediT authorship contribution statement

He Yao: Methodology, Investigation, Formal analysis, Data curation. **Wenhao Ji:** Writing – original draft, Investigation, Formal analysis, Data curation. **Yi Feng:** Formal analysis, Data curation. **Chunbo Qian:** Writing – review & editing, Investigation. **Chengguang Yue:** Writing – review & editing, Formal analysis, Data curation. **Yue Wang:** Validation, Resources, Conceptualization. **Shouying Huang:** Visualization, Validation, Conceptualization. **Mei-Yan Wang:** Writing – review & editing, Writing – original draft, Visualization, Validation, Supervision, Project administration, Methodology, Funding acquisition, Formal analysis, Conceptualization. **Xinbin Ma:** Supervision, Project administration, Conceptualization.

Acknowledgments

Financial support was received from the National Key R&D Program of China (No. 2022YFB4101900), National Natural Science Foundation of China (Nos. 22278305, U21B2096) and Natural Science Foundation of Tianjin City (No. 23JCZDJC00040).

Supplementary materials

Supplementary material associated with this article can be found, in the online version, at doi:10.1016/j.cclet.2024.110076.

References

[1] J. Artz, T.E. Müller, K. Thenert, et al., Chem. Rev. 118 (2018) 434–504.
[2] K. Dong, X.F. Wu, Angew. Chem. Int. Ed. 56 (2017) 5399–5401.
[3] M. Aresta, A. Dibenedetto, A. Angelini, Chem. Rev. 114 (2014) 1709–1742.
[4] B. Chen, M. Dong, S. Liu, et al., ACS Catal. 10 (2020) 8557–8566.
[5] A. Banerjee, G.R. Dick, T. Yoshino, et al., Nature 531 (2016) 215–219.
[6] M.Y. Wang, X. Jin, X. Wang, et al., Angew. Chem. Int. Ed. 60 (2021) 3984–3988.
[7] Q. Cheng, M. Huang, Q. Ye, et al., Chin. Chem. Lett. 35 (2024) 109112.
[8] M. Zhu, L. Zhang, S. Liu, et al., Chin. Chem. Lett. 31 (2020) 1961–1965.
[9] M.U. Khan, S.U. Khan, J. Kiriratnikom, et al., Chin. Chem. Lett. 33 (2022) 1081–1086.
[10] X. He, L.Q. Qiu, W.J. Wang, et al., Green Chem. 22 (2020) 7301-7320.
[11] T. Ju, Y.Q. Zhou, K.G. Cao, et al., Nat. Catal. 4 (2021) 304–311.
[12] X. Wang, M. Nakajima, R. Martin, J. Am. Chem. Soc. 137 (2015) 8924–8927.
[13] T. Fujihara, Y. Tani, K. Semba, et al., Angew. Chem. Int. Ed. 51 (2012) 11487–11490.
[14] T. Ohishi, L. Zhang, M. Nishiura, et al., Angew. Chem. Int. Ed. 50 (2011) 8114–8117.
[15] H. Yao, M.Y. Wang, C.G. Yue, et al., Trans. Tianjin Univ. 29 (2023) 254–274.
[16] A. Gevorgyan, K.H. Hopmann, A. Bayer, ChemSusChem 13 (2020) 2080–2088.
[17] A. Tortajada, R. Ninokata, R. Martin, J. Am. Chem. Soc. 140 (2018) 2050–2053.
[18] M. Takimoto, M. Mori, J. Am. Chem. Soc. 123 (2001) 2895–2896.
[19] H. Li, J. Long, Y. Li, et al., Eur. J. Org. Chem. 2021 (2021) 1424–1428.
[20] Y.Y. Gui, N. Hu, X.W. Chen, et al., J. Am. Chem. Soc. 139 (2017) 17011–17014.
[21] Y.Y. Gui, X.W. Chen, X.Y. Mo, et al., J. Am. Chem. Soc. 146 (2024) 2919–2927.

[22] X.W. Chen, L. Zhu, Y.Y. Gui, et al., J. Am. Chem. Soc. 141 (2019) 18825–18835.
[23] A.M. Sheta, M.A. Mashaly, S.B. Said, et al., Chem. Sci. 11 (2020) 9109–9114.
[24] S. Dérien, J.C. Clinet, E. Duñach, et al., Tetrahedron 48 (1992) 5235–5248.
[25] J. Bringmann, E. Dinjus, Appl. Organomet. Chem. 15 (2001) 135–140.
[26] C. Zhou, X. Wang, L. Yang, et al., Green Chem. 24 (2022) 6100-6107.
[27] P. Zhang, Z. Zhou, R. Zhang, et al., Chem. Commun. 56 (2020) 11469–11472.
[28] Y. Hu, L. Hu, H. Gao, et al., Org. Chem. Front. 9 (2022) 2240–2248.
[29] W. Hang, S. Zou, C. Xi, ChemCatChem 11 (2019) 3814–3817.
[30] J. Takaya, K. Sasano, N. Iwasawa, Org. Lett. 13 (2011) 1698–1701.
[31] M. Juhl, S.L.R. Laursen, Y. Huang, et al., ACS Catal. 7 (2017) 1392–1396.
[32] L. Zhang, J. Cheng, B. Carry, et al., J. Am. Chem. Soc. 134 (2012) 14314–14317.
[33] H. Ohmiya, M. Tanabe, M. Sawamura, Org. Lett. 13 (2011) 1086–1088.
[34] S.S. Yan, D.S. Wu, J.H. Ye, et al., ACS Catal. 9 (2019) 6987–6992.
[35] M. Magre, M. Szewczyk, M. Rueping, Chem. Rev. 122 (2022) 8261–8312.
[36] J.H. Docherty, J. Peng, A.P. Dominey, et al., Nat. Chem. 9 (2017) 595–600.
[37] F. Meng, H. Jang, B. Jung, et al., Angew. Chem. Int. Ed. 52 (2013) 5046–5051.
[38] F. Meng, F. Haeffner, A.H. Hoveyda, J. Am. Chem. Soc. 136 (2014) 11304–11307.
[39] H. Pang, D. Wu, G. Yin, Chin. J. Org. Chem. 41 (2021) 849–856.
[40] H. Pang, D. Wu, H. Cong, et al., ACS Catal. 9 (2019) 8555–8560.
[41] T.M. Perrone, A.S. Gregory, S.W. Knowlden, et al., ChemCatChem 11 (2019) 5814–5820.
[42] X. Lv, Y.B. Wu, G. Lu, Catal. Sci. Technol. 7 (2017) 5049–5054.
[43] S. Zhang, L. Li, D. Li, et al., J. Am. Chem. Soc. 146 (2024) 2888–2894.
[44] J. Rae, K. Yeung, J.J.W. McDouall, et al., Angew. Chem. Int. Ed. 55 (2015) 1102–1107.
[45] W. Jian, M.F. Chiou, Y. Li, et al., Chin. Chem. Lett. 35 (2024) 108980.
[46] X.Y. Chen, X. Zhou, J. Wang, et al., ACS Catal. 10 (2020) 14349–14358.
[47] C.X. Liu, Q. Gu, S.L. You, Trends Chem. 2 (2020) 737–749.
[48] H. Zhao, Z. Lin, T.B. Marder, J. Am. Chem. Soc. 128 (2006) 15637–15643.
[49] L. Dang, H. Zhao, Z. Lin, et al., Organometallics 26 (2007) 2824–2832.
[50] L. Dang, Z. Lin, T.B. Marder, Organometallics 29 (2010) 917–927.
[51] N.N. Baughman, N.G. Akhmedov, J.L. Petersen, et al., Organometallics 40 (2021) 23–37.
[52] M.F. Obst, A. Gevorgyan, A. Bayer, et al., Organometallics 39 (2020) 1545–1552.
[53] J. Ruan, J.A. Iggo, N.G. Berry, et al., J. Am. Chem. Soc. 132 (2010) 16689–16699.
[54] X. Guo, T. Wang, Y. Zheng, et al., J. Organomet. Chem. 904 (2019) 121014.
[55] X. Li, H. Wu, Z. Wu, et al., J. Org. Chem. 84 (2019) 5514–5523.
[56] J. Liu, W. Nie, H. Yu, et al., Org. Biomol. Chem. 18 (2020) 9065–9071.
[57] D. García-López, L. Pavlovic, K.H. Hopmann, Organometallics 39 (2020) 1339–1347.
[58] A. Sengupta, B. Li, D. Svatunek, et al., Acc. Chem. Res. 55 (2022) 2467–2479.
[59] F.M. Bickelhaupt, K.N. Houk, Angew. Chem. Int. Ed. 56 (2017) 10070–10086.
[60] D.S. Laitar, P. Müller, J.P. Sadighi, J. Am. Chem. Soc. 127 (2005) 17196–17197.
[61] C. Borner, L. Anders, K. Brandhorst, et al., Organometallics 36 (2017) 4687–4690.
[62] S.H. Newman-Stonebraker, S.R. Smith, J.E. Borowski, et al., Science 374 (2021) 301–308.
[63] H. Clavier, S.P. Nolan, Chem. Commun. 46 (2010) 841–861.
[64] K. Wu, A.G. Doyle, Nat. Chem. 9 (2017) 779–784.
[65] L. Falivene, R. Credendino, A. Poater, et al., Organometallics 35 (2016) 2286–2293.
[66] T.P. Moneypenny, A. Yang, N.P. Walter, et al., J. Am. Chem. Soc. 140 (2018) 5825–5833.